Chapter 5

Transcriptomic Analysis of *Escherichia coli K12* under the Exposure of Lysozyme coated Silver Nanoparticles

- This work was carried out under EMBO Short-Term Fellowship (ESTF 7654) awarded to me to work in the laboratory of Prof. Sèamus Fanning at UCD-Center for Food Safety, University College Dublin, Dublin (October-December 2018).

5.1 Introduction

With the beginning of antibiotic era, the overdose and lack of knowledge about the consumption of antibiotics have pushed the rapid advent of multidrug-resistance (MDR) pathogens (Niu and Li, 2019). MDR is defined as the insensitivity or resistance of any microorganism to various antibiotics to which they were earlier sensitive (Nikaido, 2009; Medina and Pieper, 2016). Development of MDR in pathogenic bacteria is a major problem in the current medicine because it leads to higher mortality, morbidity and elevated healthcare costs (Medina and Pieper, 2016). Generation of resistance against most effective antibiotics has driven the need for the search and development of new antibacterial agents (Aslam et al., 2018).

As discussed in previous chapters, different forms of silver exert robust antibacterial potential, which makes it a potential antibacterial candidate against MDR pathogens. Antibacterial potential of silver in its ionic and nano forms has been discussed in previous chapters. Moreover, the quantitative real-time polymerase chain reaction (qRT-PCR) was used to study the differential gene expression profiling of *Escherichia coli* K12 exposed to silver species. In Chapter 4, we have discussed the mechanistic differences in the antibacterial activity of the silver ions and Ag NPs. The lysozyme coated silver nanoparticles (L-Ag NPs) were observed to act as reservoir and slowly release silver ions which results in differential expression of selected genes. The maximum change in the gene expression profiling was observed when *E. coli* cells were exposed to MIC_{75} concentration [6.75 µg (Ag) mL^{-1}] of tested silver species. However, the convenient toxicity assays and qRT-PCR analysis of a few selected genes may not suffice to fully capture the complexities of cellular response towards Ag NPs. New and more comprehensive approach such as RNA sequencing (RNAseq) is needed to understand all the metabolic pathways, signaling and molecular functions in bacterial cells exposed to Ag NPs. RNAseq has been utilized in recent years to study the complete transcriptome of prokaryotic and eukaryotic cells (Wang et al., 2009; Croucher and Thomson, 2010; Feliu et al., 2014; Sun et al., 2017; Lowe et al., 2017). This technique is used to study the complete transcriptome of an organism viz. the sum of all the RNA transcripts. In comparison to the second generation sequencing technique such as microarray, which measures the abundance of a defined set of transcripts via their hybridisation of complementary probes (Schena et al., 1995), the next generation RNAseq technique denotes the sequencing of transcript cDNAs, in which abundance is derived from the number of counts from each transcript (Wang et al., 2009). Out of these two techniques, RNA sequencing is known to be

more accurate because of several reasons viz. higher specificity and sensitivity, simple detection of rare and low-abundance transcripts, capability to spot novel transcripts, and wider dynamic range (Zhao et al., 2014; Wang et al., 2014; Liu et al., 2015). RNAseq has been utilized in various studies to study the bacterial transcriptome under different stress conditions like NPs, antibiotics, antibacterial agents, etc. (Sun et al., 2017; Anes et al., 2019).

This chapter discusses the whole transcriptome profiling of *E. coli* K12 exposed to MIC_{75} concentration of L-Ag NPs for 5 and 30 min., by RNAseq.

5.2 Material and methods

5.2.1 Materials

All chemicals used for antibacterial activity assays (except Ag NPs) were of analytical grade and purchased from Sigma Aldrich (USA) unless otherwise stated. Milli-Q water was acquired from a Milli- Millipore (Merck KGaA, Darmstadt, Germany).

5.2.2 Preparation of bacterial culture and exposure to L-Ag NPs

E. coli K12 was revived from the glycerol stock and cultured in MLB broth medium (casein enzyme hydrolysate 10 g L^{-1} and yeast extract 5 g L^{-1}, pH 7.2 ± 0.2) for 12 h at 37°C under shaking (150 rpm). For preparation of inoculum, overnight grown bacterial culture was inoculated in freshly prepared MLB medium and allowed to raise till the log phase (OD_{600} 0.5-0.6). Freshly grown *E. coli* K12 cells (~ 3×10^7 CFU mL^{-1}) were exposed to MIC_{75} concentration [6.75 µg (Ag) mL^{-1}] of L-Ag NPs for 5 and 30 min. at 37°C in MLB broth, separately. Bacterial cells without any treatment of L-Ag NPs served as a control for each time point.

5.2.3 RNA sequencing analysis

Based on the results obtained during the gene expression analysis studies discussed in Chapter 4, as maximum changes were observed only at 5 and 30 min time points, these time points were selected for the transcriptomic analysis studies. Samples of the bacterial culture were taken at 5 and 30 min. post L-Ag NPs exposure by separating the bacterial cells after washing thrice using phosphate buffer (pH 7.2). RNA was isolated from the bacterial pellet using RNAeasy extraction kit (Qiagen, Hilden, Germany) following manufacturer's instructions. In order to remove any DNA contamination, the isolated RNA was treated with Turbo DNase kit (Ambion's, USA). Integrity of the DNase treated RNA was checked by the

Bioanalyzer 2100 RNA 6000 nanochip (Agilent Technologies, United States) and the purified RNA samples were stored at -80°C until further use.

The RNA library preparation and subsequent sequencing were outsourced from Centre for Genomic Research, University of Liverpool, UK and in total 8 libraries were prepared as per the details given in the Table 5.1. For the removal of ribosomal RNA, Ribo-Zero rRNA removal kit (Illumina, USA) was used, as per the manufacturer's instruction. For the preparation of libraries from purified RNA sample, NEBNext® Directional RNA Library Prep Kit (New England BioLabs, Germany) was used. Pooled libraries were loaded on cBot (Illumina, USA) and cluster generations was performed as per the manufacturer's instructions. single-end sequencing 150 bp read length was performed on lane of the HiSeq 4000 sequencer (Illumina, USA).

Table 5.1: Overview of the RNA sequencing libraries for *E. coli* K12.

S. no.	Name of library	Treatment time
1.	Control 5 min. (Replicate 1)	5 min.
2.	Control 5 min. (Replicate 2)	
3.	Test 5 min. (Replicate 1)	
4.	Test 5 min. (Replicate 2)	
5.	Control 30 min. (Replicate 1)	30 min.
6.	Control 30 min. (Replicate 2)	
7.	Test 30 min. (Replicate 1)	
8.	Test 30 min. (Replicate 2)	

Ra

research group (Anes et al., 2019). Briefly, RTA version 1.18.61 was used for the processing of raw sequencing data and CASAVA 1.8.4 was used to generate FASTQ-files. All the sequences were mapped against reference genome of *E. coli* K12 (NC_000913.3) using Segemehl with an accuracy of 100 % (Hoffmann et al., 2009; Anes et al., 2019) and uniquely mapped reads were used for the computational analysis. R (version 3.2.4) programme was used for the computational analysis of RNAseq data. To get the expression level of genes, *VOOM* function (Law et al., 2014) in the *limma* package (Ritchie et al., 2015) was used to normalize the raw read counts. To make it more precise, counts were converted to $\log_2$ counts per million followed by fitting the linear model to each gene. Empirical Bayes moderated t-statistics and its corresponding P-values were used to access the differences in expression of genes (Smyth et al., 2005; Law et al., 2014). Benjamini–Hochberg corrected P-values were used for the

computing of multiple comparisons. Gene ontology (GO) enrichment pathway and GO biological processes (GOBP) terms analysis of differentially expressed genes was performed using GOseq R package. GO enrichment pathway analysis was performed separately for the samples taken at 5 and 30 min. post L-Ag NPs exposure, with a False Discovery Rate (FDR) value at $p \leq 0.05$ (adjacent p value).

The qRT-PCR results of selected genes (*soxS*, *cusC*, *copA*, *sufB*, *recA*, and *dnaK*) as detailed in Chapter 4 were used to validate the RNAseq data.

5.2.4 Transmission electron microscopy

Transmission Electron Microscopy (TEM) measurements were carried out to determine the morphology of the bacteria after the L-Ag NP treatment. In order to prepare sample for TEM analysis, the bacterial cells exposed to MIC_{75} concentration of L-Ag NPs for 30 min. was centrifuged at 8,000 rpm for 10 min. Subsequently, the supernatant was discarded, and the pellet was washed twice with 1X Phosphate Buffer Saline (PBS) buffer followed by their fixation in 2.5% electron microscopy grade glutaraldehyde (prepared in 0.05 M sodium cacodylate buffer; pH 7.2) for 2 h at 4°C. After fixation, the cells were washed thrice with cacodylate buffer (without glutaraldehyde) and were resuspended in the same buffer. The TEM samples were prepared by drop-casting the bacterial cell suspension on a carbon-coated copper grid. The cells not exposed to L-Ag NPs were used as the control. The prepared grids were observed on a Hitachi H-7650 TEM instrument (Hitachi High-Technologies Corporation, Japan) at an acceleration voltage of 100 kV. Elemental analysis of bacterial samples was carried out using a Quantax EDS attachment (Bruker AXS Ltd., Coventry, UK) equipped with TEM.

5.2.5 Statistical analysis

The qRT-PCR measurements data were statistically analysed using Prism software (Version 8.0; GraphPad Software Inc.) (Motulsky, 1999). All the data points represent the mean of two independent measurements unless otherwise stated. The uncertainties were represented as standard deviations. In RNAseq results, NSE represents non-significant expression.

5.3 Results and Discussion

5.3.1 RNA sequencing analysis

In order to decipher the complete mechanistic insights of antibacterial action of L-Ag NPs on *E. coli* K12, whole transcriptome was analysed by high throughput RNAseq analysis. Bacterial cells were exposed to MIC_{75} concentration [6.75 µg (Ag) mL^{-1}] of L-Ag NPs for 5

and 30 min. The time points for the treatment were selected based on the bacterial replication time of *E. coli* (~ 20 min.) (Chandler et al., 1975; Skarstad et al., 1986). The 5 min. time point was used to identify the early transcriptional signals following L-Ag NPs exposure, whereas the 30 min. time point was used to identify the adaptive responses as by this time one replication cycle was already completed in the *E. coli* K12 cells. Bacteria without any L-Ag NPs treatment was used as a control for each time point. RNAseq raw data provided about 310 million reads across all the 8 libraries with an average of 38.75 million reads per library which is a significant number for the transcriptomic analysis in *E. coli* (Haas et al., 2012).

Differential expression of all the genes of *E. coli* K12 was identified using *VOOM* function in the *limma* package (Ritchie et al., 2015). Differential gene expression was obtained for total 4344 genes upon exposure of *E. coli* K12 to L-Ag NPs for 5 and 30 min. time points. Among all the differentially expressed genes, statistically significant genes were selected by setting FDR (false discovery rate) value at $p \leq 0.05$ (adjacent p value) (Anes et al., 2019). Out of 4344 genes, 2164 and 2285 genes were found to be statistically significant at 5 min. and 30 min. time points, respectively (Figure 5.1). Genes with a $\log_2$ fold change value of ≥ 1.0 and ≤ -1.0 were considered to be up-regulated and down regulated, respectively (Dash et al., 2018; Anes et al., 2019). On this basis, 238 genes were found to be up-regulated, 193 genes were down regulated, and 1733 genes remained neutral at 5 min. post L-Ag NPs exposure. However, at 30 min. treatment, 340 genes were found to be up-regulated, 205 genes got down-regulated, and 1740 genes were found to remain neutral (Figure 5.2).

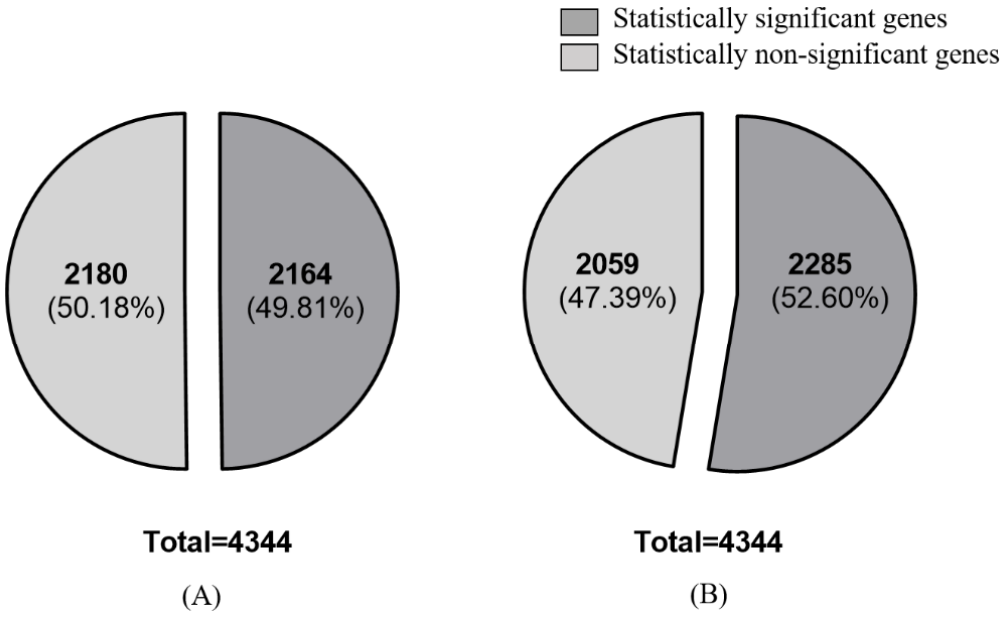

Figure 5.1: Overview of statistically significant and non-significantly expressed (NSE) genes at (A) 5 min. and (B) 30 min., post L-Ag NPs exposure (FDR, $p \leq 0.05$).

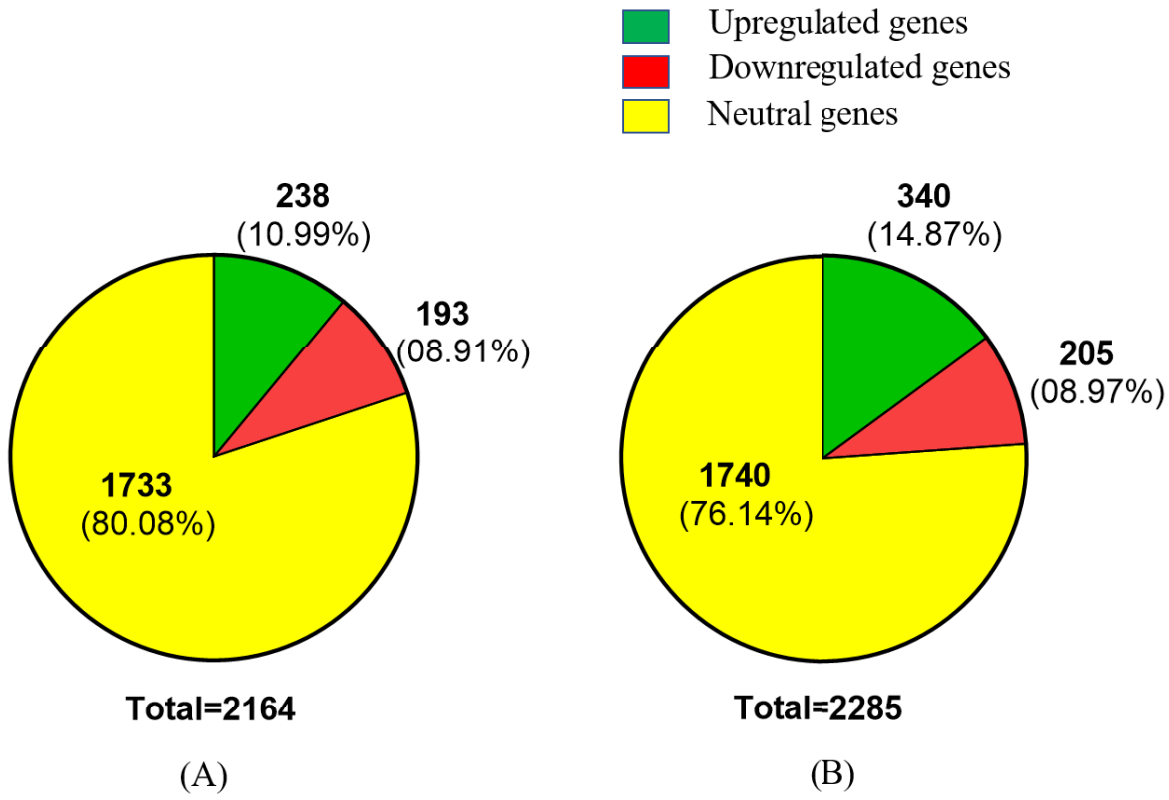

Figure 5.2: Overview of significantly expressed genes at (A) 5 min., and (B) 30 min. post L-Ag NPs exposure.

Among all the up-regulated genes at 5 and 30 min. post L-Ag NPs exposure, 138 genes were found to be commonly up-regulated, whereas 100 and 202 genes were specifically up-regulated at 5 min. and 30 min., respectively. In case of down-regulated genes, 29 genes were found to be commonly down-regulated at both time points whereas, 164 and 176 genes were specifically down-regulated at 5 min. and 30 min. treatment. Total 957 genes were commonly found in neutral category (Figure 5.3).

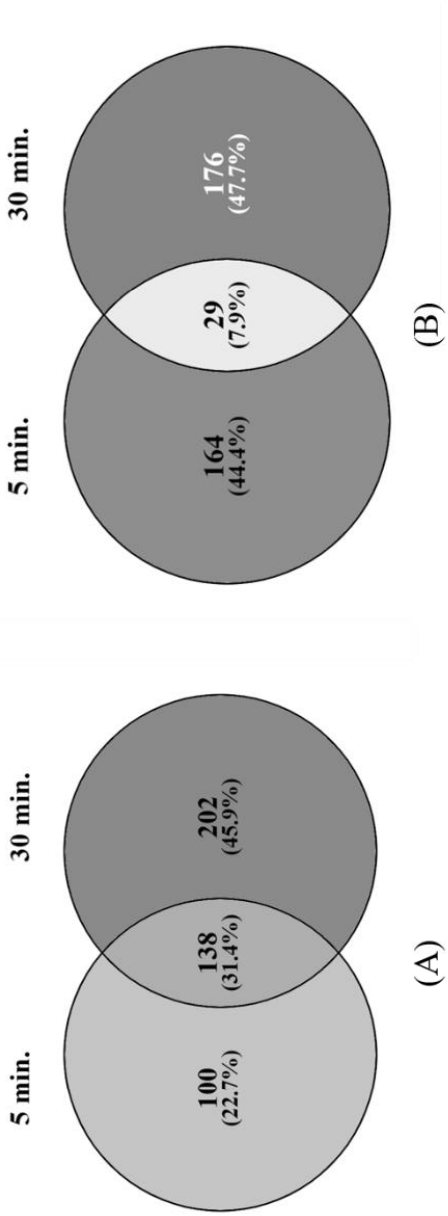

Figure 5.3: Venn diagram showing overlapping sets of differentially (A) up-regulated, (B) down-regulated and (C) neutral genes at 5 and 30 min. post L-Ag NPs exposure

In the present study, differential expression pattern of genes probably involved in the antibacterial activity of Ag NPs was analysed. As discussed in Chapter 4, bacterial envelope of Gram-negative bacteria is made up of three different layers viz. outer membrane lipopolysaccharide (LPS), peptidoglycan cell wall, and plasma membrane. The silver ions released from the L-Ag NPs first encounter the outer membrane of *E. coli*, through which they can enter into the bacterial cell. As mentioned in Chapter 4, ions released from NPs can enter the bacterial cells either by damaging the bacterial outer membrane or through the porin proteins. Hence, we have considered the outer membrane (LPS) for the differential gene expression study because it is utmost necessity for any antibacterial agent to interact with LPS,

in order to invade the bacterial envelope (May and Grabowicz, 2018). In the present study, the LPS synthesis genes were investigated to check the membrane damage which eventually allow the entry of silver ions into the bacterial cells. Differential expression pattern of genes related to the LPS synthesis did not show any sign of membrane damage as most of the genes were found to be neutral and many of them showed statistically non-significant expression (NSE), which suggest that silver ions could not damage the bacterial outer membrane (Table 5.2). In case of membrane damage, downregulation of LPS synthesis genes would have been observed due to the activation of alternate sigma factor (σ^{30}) (Rhodius et al., 2005).

Table 5.2: Differential expression profile of lipopolysaccharide biosynthesis regulating genes under the stress of L-Ag NPs.

Gene ID	Gene name	Log_2 fold change		Protein annotation
		5 min.	30 min.	
b3633	*waaA*	-0.49473	NSE	KDO transferase
b3628	*waaB*	NSE	-0.37134	UDP-D-galactose:(glucosyl) lipopolysaccharide-1,6-D-galactosyltransferase
b3622	*waaL*	-0.25949	-0.91752	O-antigen ligase
b3627	*waaO*	NSE	-0.37652	UDP-D-glucose:(glucosyl) LPS alpha-1,3-glucosyltransferase
b3630	*waaP*	-0.27254	-0.36689	Lipopolysaccharide core heptose (I) kinase
b3632	*waaQ*	-0.19161	-0.21293	Lipopolysaccharide core heptosyltransferase 3
b3625	*waaY*	NSE	-0.45622	Lipopolysaccharide core heptose (II) kinase
b3624	*waaZ*	NSE	-0.55744	Lipopolysaccharide core biosynthesis protein WaaZ
b2035	*wbbH*	-0.22851	-0.72371	Putative O-antigen polymerase
b3546	*eptB*	1.176718	1.663687	Kdo2-lipid A phosphoethanolamine 7''-transferase
b3955	*eptC*	-0.16907	-0.83346	Phosphoethanolamine transferase EptC

b0181	*lpxA*	-0.32095	-0.36581	UDP-N-acetylglucosamine acyltransferase
b0182	*lpxB*	-0.31884	NSE	Lipid A disaccharide synthase
b0096	*lpxC*	0.328025	0.505181	UDP-3-O-acyl-N-acetylglucosamine deacetylase
b0179	*lpxD*	NSE	-0.14247	UDP-3-O-(3-hydroxymyristoyl) glucosamine N-acyltransferase
b1054	*lpxL*	-0.26021	NSE	Lauroyl acyltransferase

To check another pathway for the entry of silver ions into bacterial cell, the genes related to the synthesis of porin proteins were analysed. Differential expression analysis confirmed the action of L-Ag NPs by releasing silver ions which entered inside the bacterial cell. Out of various genes regulating the biosynthesis of porin proteins, significant down-regulation of *ompF* was observed at 30 min. time point (Table 5.3). This suggests that silver ions released from L-Ag NPs could enter in the cells through these proteins. OmpF porin protein is among the two major porin proteins along with OmpC which are known to allow the passive diffusion of small cationic molecules into the bacterial cell (Lou et al., 1996; Nikaido, 2003; Vergalli et al., 2019). Jaffe et al., (1982) reported the entry of β-lactam antibiotics through OmpF and OmpC porin proteins in *E. coli* K12, as mutants of these proteins found to be resistant against β-lactam antibiotics. In addition, entry of colicin toxins in bacteria has reported to be mediated through OmpF porin proteins (Cramer et al., 2018). The down-regulation in the expression of *ompF* gene suggest that by 30 min. time point the bacterial defence system get activated to restrict further entry of cationic silver ions through OmpF porin proteins. However, no significant change in the expression pattern of aquaporin *aqpZ* gene was observed at both 5 and 30 min. time points which validates the results obtained by qRT-PCR analysis. Wei et al. (2001) also reported that *aqpZ* gene does not express in present of LB medium.

Table 5.3: Differential expression profile of porin protein biosynthesis regulating genes under the stress of L-Ag NPs.

Gene ID	**Gene name**	**Log_2 fold change**		**Protein annotation**
		5 min.	**30 min.**	
b0957	*ompA*	-0.18162	-0.67158	Outer membrane porin A
b2215	*ompC*	NSE	-0.46774	Outer membrane porin C
b0929	*ompF*	-0.30075	-4.1133	Outer membrane porin F

b0814	*ompX*	NSE	0.170518	Outer membrane protein X
b0875	*aqpZ*	0.325802	0.553863	Water channel AqpZ
b0553	*nmpC*	NSE	-1.21333	DLP12 prophage%3B putative outer membrane porin NmpC
b2250	*yfaZ*	-0.33354	0.488169	Putative porin YfaZ

Analysis of outer membrane and porin proteins genes confirmed the results discussed in Chapter 4 about the entry of L-Ag NPs into the bacterial cell. L-Ag NPs did not damage the bacterial membrane, instead they act as reservoir and release silver ions in the proximity to the bacteria, and these silver ions subsequently get into the bacteria through porin proteins.

As discussed in Chapter 4, upon entry of silver ions inside bacterial cells they result in the generation of reactive oxygen species (ROS). In order to find out which kind of ROS has been generated, different ROS generating mechanisms were analysed by studying differential expression of ROS regulating genes under the stress of L-Ag NPs (Table 5.4). The obtained results showed an up-regulation in the *sodA* gene encoding superoxide dismutase and *katE* gene encoding catalase by ~1.6 and ~2.0 $\log_2$ fold change at 30 min. post L-Ag NPs exposure. It is well known that in order to circumvent the ROS generated in the form of H_2O_2, the bacteria up-regulate the superoxide dismutase and catalase enzymes which are used to scavenge the H_2O_2 free radicals (Imlay, 2008). This increase in the ROS generation can be directly correlated with the stress sensed by the bacterial cell, which in turn activates the bacterial defence mechanism to counter the stress.

Table 5.4: Differential expression profile of ROS regulating genes under the stress of L-Ag NPs.

Gene ID	**Gene name**	**Log_2 fold change**		**Protein annotation**
		5 min.	**30 min.**	
b3908	*sodA*	0.274355	1.602584	Superoxide dismutase (Mn)
b1656	*sodB*	0.164487	-0.63923	Superoxide dismutase (Fe)
b1646	*sodC*	0.302951	NSE	Superoxide dismutase (Cu-Zn)
b1732	*katE*	1.810638	2.002176	Catalase II
b3942	*katG*	-0.77732	1.000623	Hydroperoxidase I

b0605	*ahpC*	-0.37084	0.876958	Alkyl hydroperoxide reductase, AhpC component
b0475	*hemH*	-0.29368	0.368581	Ferrochelatase
b0849	*grxA*	-1.027	0.794609	Reduced glutaredoxin 1
b1064	*grxB*	0.530768	NSE	Reduced glutaredoxin 2
b3610	*grxC*	0.254498	-0.23262	Glutaredoxin 3
b1654	*grxD*	NSE	0.158355	Glutaredoxin 4
b1635	*gstA*	NSE	0.64149	Glutathione S-transferase GstA
b0838	*gstB*	NSE	0.488429	Glutathione S-transferase GstB
b3781	*trxA*	0.295829	NSE	Thioredoxin 1
b0888	*trxB*	-0.27419	0.13722	Thioredoxin reductase
b2582	*trxC*	-0.46242	0.435212	Reduced thioredoxin 2
b3860	*dsbA*	0.630908	2.023092	Thiol:disulfide oxidoreductase DsbA
b0604	*dsbG*	0.352225	NSE	Protein sulfenic acid reductase DsbG

Complete mechanism for the regulation of oxidative stress regulation in *E. coli* has been discussed in Chapter 4. In brief, *E. coli* has two defence regulatory mechanisms viz. OxyR and SoxRS system. Out of these two systems, SoxRS has been reported to be more dominant in *E. coli* under the oxidative stress (Gaudu et al., 1997; Pomposiello and Demple, 2001; Seo et al., 2015). This system comprised of two main proteins SoxR and SoxS encoded by *soxR* and *soxS* genes, respectively. SoxR protein has a constitutive expression in bacterial cell under normal conditions, whereas SoxS protein is a response of activation of defence system under redox stress (Pomposiello and Demple, 2001). Under oxidative stress condition, *E. coli* K12 induces production of around 80 polypeptides and the synthesis of these polypeptides are controlled by the *soxRS* regulon at the transcriptional level (Pomposiello and Demple, 2001). Differential analysis of genes related to OxyR and SoxRS systems showed that expression of *soxS* was maximum (3.99 $\log_2$ fold up-regulation) among all the genes and remained almost same at both time points (Table 5.5). The obtained results confirmed that soxRS machinery is mainly responsible for the regulation of oxidative stress upon exposure to L-Ag NPs. Constant expression of *soxS* showed that bacteria could sense the stress conditions of silver ions at the initial time point (5 min.) and activated its defence mechanism upon the completion of one replication cycle which prevented further up-regulation in the expression of *soxS*. Similar kind of results were reported by McQuillan et al. (2014). They treated *E. coli* with silver species

only for 10 min. and found the active involvement of soxRS regulon in the oxidative stress sensing.

Table 5.5: Differential expression profile of genes related to bacterial defence under the stress of L-Ag NPs.

Gene ID	Gene name	Log_2 fold change		Protein annotation
		5 min.	30 min.	
b4063	*soxR*	-0.62969	-0.5524	DNA-binding transcriptional dual regulator SoxR
b4062	*soxS*	3.992345	3.96795	DNA-binding transcriptional dual regulator SoxS
b3961	*oxyR*	1.334427	1.053249	DNA-binding transcriptional dual regulator OxyR
b4458	*oxyS*	-0.84871	NSE	Small regulatory RNA OxyS
b3924	*fpr*	1.248349	2.203978	Flavodoxin/ferredoxin-NADP(+) reductase

As discussed in Chapter 4, *E. coli* is a peritrichous flagellar bacteria and these flagella are actively involved in the motility, biofilm formation and attachment to the host surface. Synthesis of bacterial flagella and its role in motility are highly controlled processes and their regulation occurs at various levels viz. transcriptional, post-transcriptional, etc. (Liu and Ochman, 2007). It is a known fact that flagella are the outermost bacterial moiety on the *E. coli* cell and upon exposure of any antibacterial agent, their first interaction occur with the bacterial flagella. Changes in the expression of genes related to the functioning of flagella would be important to decipher the molecular mechanism of L-Ag NPs. Keeping the above facts in mind, differential gene regulation of genes related to the flagella synthesis and maintenance were taken into consideration. Transcription factor FlhDC is the master regulator of flagellar network in *E. coli* and other related *Enterobacteriaceae* bacterial species (Soutourina and Bertin, 2003). Expression and functioning of FlhDC operon is regulated at several levels, which makes it responsible for the activation of all the structural and functional components of flagellar molecular machinery. In general, FlhDC activates seven different commonly accepted operons which further includes various genes (Fitzgerald et al., 2014) (Table 5.6).

Table 5.6: Differential expression profile of genes related to flagella biosynthesis under the stress of L-Ag NPs.

Gene ID	Gene name	Log_2 fold change		Protein annotation
		5 min.	30 min.	
b1880	*flhB*	NSE	-1.79393	Flagellar biosynthesis protein FlhB
b1891	*flhC*	-1.27384	-3.01191	DNA-binding transcriptional dual regulator FlhC
b1892	*flhD*	-1.22159	-2.82529	DNA-binding transcriptional dual regulator FlhD
b1922	*fliA*	-0.77968	-2.6868	RNA polymerase, sigma 28 (sigma F) factor
b1923	*fliC*	0.272837	NSE	Flagellar filament structural protein
b1937	*fliE*	NSE	-3.20646	Flagellar basal-body protein FliE
b1938	*fliF*	NSE	-3.225	Flagellar basal-body MS-ring and collar protein
b1939	*fliG*	NSE	-1.9296	Flagellar motor switch protein FliG
b1944	*fliL*	NSE	-3.56819	Flagellar protein FliL
b1945	*fliM*	NSE	-3.17954	Flagellar motor switch protein FliM
b1946	*fliN*	NSE	-3.12436	Flagellar motor switch protein FliN
b1947	*fliO*	NSE	-3.43543	Flagellar biosynthesis protein FliO
b1073	*flgB*	NSE	-3.42313	Flagellar basal-body rod protein FlgB
b1074	*flgC*	NSE	-3.20304	Flagellar basal-body rod protein FlgC
b1075	*flgD*	NSE	-3.32489	Flagellar biosynthesis, initiation of hook assembly
b1272	*sohB*	NSE	0.218724	S49 peptidase family protein
b1271	*yciK*	0.670348	1.033884	Putative oxidoreductase
b1890	*motA*	NSE	-1.86801	Motility protein A
b1889	*motB*	NSE	-1.0841	Motility protein B

Differential expression analysis of all the genes involved in the synthesis of flagella showed that at initial 5 min. time point, L-Ag NPs could not disturb the flagellar synthesis and bacterial motility as only *FlhD* and *FlhC* got differentially regulated with -1.22 and -1.27 log_2 fold change, respectively. However, at 30 min. time point of L-Ag NPs, drastic change has been observed in the gene expression analysis where, *FlhD* and *FlhC* were down-regulated to -2.82 and -3.01 log_2 fold change, respectively. Along with FlhDC operons, many other genes also got down-regulated at 30 min. time point (Table 5.6). In general, biosynthesis of flagella is an energy consuming process. Hence, in adverse conditions, when the growth potential of bacteria decreases, it down-regulates the biosynthesis of flagella in order to save energy to survive under adverse conditions (Zhao et al., 2007). Spöring et al. (2018) studied the expression of flagellar biosynthesis genes in the lipopolysaccharide (LPS) truncated mutants

of *Salmonella typhimurium* and reported that bacteria firmly down-regulates the flagellar biosynthesis under unfavourable conditions, which results in the disturbance in the sigma factor and activation of alternative sigma factor (σ^{24}), that usually occurs under the oxidative stress (Kazmierczak et al., 2005). This study revealed the down-regulation of flagellar biosynthesis genes specifically FlhDC operons which suggests the energy saving behaviour of bacteria under adverse conditions. Likewise, decrease in the expression of genes specifically related to the flagellar regulation were observed under the exposure of L-Ag NPs which might be a strategy to survive under the oxidative stress conditions.

Now a question arises that whether these changes in the bacterial functioning under the stress of L-Ag NPs affect the DNA/ protein processing or not? To check these aspects, we have analysed differential expression of genes related to the DNA and protein repair machinery. In this regard, SOS response machinery and protein chaperones were analysed, as discussed in Chapter 4. In general, oxidative stress causes damage in the bacterial DNA depending on the type, concentration and exposure time of antibacterial agents (Gruber and Walker, 2018). Differential expression analysis showed that DNA processing was not much affected upon exposure of bacterial cells to MIC_{75} concentration of L- Ag NPs, as no significant change in the expression pattern of genes related to the DNA repair machinery were observed (Table 5.7). However, the expression profile of protein chaperones showed significant up-regulation of various chaperones, which were found to be maximum at the initial time point (5 min.) and decreased at the later time point (30 min.). This may be due to the activation of bacterial defence system after completion of one replication cycle by 30 min. Maximum up-regulation was observed in the expression of *dnaK* gene with a $\log_2$ fold change value of ~2.9 and ~1.6 at 5 and 30 min. time points, respectively (Table 5.8). Increase in the expression of protein chaperones can be correlated with activation of alternative sigma factor (σ^{E}) (Kazmierczak et al., 2005). This leads to the up-regulation of molecular chaperone in order to prevent protein misfolding & aggregation, and help the bacterial cell to survive under the stress of L-Ag NPs (Rhodius et al., 2005; Rollauer et al., 2015).

Table 5.7: Differential expression profile of genes related to DNA repair mechanism under the stress of L-Ag NPs.

Gene ID	Gene name	Log_2 fold change		Protein annotation
		5 min.	30 min.	
b4043	*lexA*	0.200608	NSE	DNA-binding transcriptional repressor LexA
b2699	*recA*	0.38152	0.215317	DNA recombination/repair protein RecA
b4058	*uvrA*	0.141138	NSE	Excision nuclease subunit A
b1913	*uvrC*	-0.25661	-0.23264	Excision nuclease subunit C
b3813	*uvrD*	-0.19799	NSE	ssDNA translocase and dsDNA helicase - DNA helicase II
b1914	*uvrY*	-0.2534	-0.28458	DNA-binding transcriptional activator UvrY
b1183	*umuD*	NSE	-0.66186	DNA polymerase V protein UmuD
b1184	*umuC*	NSE	-0.76972	DNA polymerase V catalytic protein
b0060	*polB*	0.602636	NSE	DNA polymerase II
b0231	*dinB*	0.314742	NSE	DNA polymerase IV

Table 5.8: Differential expression profile of genes related to protein repair mechanism under the stress of L-Ag NPs.

Gene ID	Gene name	Log_2 fold change		Protein annotation
		5 min.	30 min.	
b4143	*groL*	2.2749433	1.54588	Chaperonin GroEL
b4142	*groS*	2.4451843	1.458124	Cochaperonin GroES
b0015	*dnaJ*	2.1447698	0.760036	Chaperone protein DnaJ
b0014	*dnaK*	2.942175	1.622535	Chaperone protein DnaK

Table 5.9: Differential expression profile of genes related to bacterial homeostasis mechanism under the stress of L-Ag NPs.

Gene ID	Gene name	Log_2 fold change		Protein annotation
		5 min.	30 min.	
b1684	*sufA*	1.560576	3.426199	Fe-S cluster insertion protein SufA
b1683	*sufB*	1.453298	3.31309	Fe-S cluster scaffold complex subunit SufB
b1682	*sufC*	1.033172	2.857299	Fe-S cluster scaffold complex subunit SufC
b1681	*sufD*	0.953068	2.647027	Fe-S cluster scaffold complex subunit SufD
b1679	*sufE*	0.466581	1.861136	Sulfur acceptor for SufS cysteine desulfurase
b1680	*sufS*	0.797758	2.463133	L-cysteine desulfurase
b2528	*iscA*	0.674354	NSE	Fe-S cluster insertion protein IscA
b2531	*iscR*	0.713797	0.38046	DNA-binding transcriptional dual regulator IscR
b2530	*iscS*	0.870857	0.257249	Cysteine desulfurase
b2529	*iscU*	0.870976	0.153813	Scaffold protein for iron-sulfur cluster assembly
b2524	*iscX*	0.3722	NSE	Accessory iron-sulfur cluster assembly protein IscX

The observed changes that occurred in the protein chaperones motivated us to check, how does bacteria maintain its cellular homeostasis under the stress of L-Ag NPs? As discussed in Chapter 4, bacterial homeostasis is maintained by the iron-sulfer cluster (ISC) system, which provides the iron sulfer complex for the functioning of various bacterial enzymes. However, IFC system doesn't work under oxidative stress conditions during which Suf system act as an alternate for the ISC system and maintain the cells homeostasis (Figure 4.13) (Outten et al., 2003; Fontecave et al., 2005). Differential expression analysis of ISC system and suf system genes was performed. No significant change in the expression of ISC system genes was observed. However, a time-dependent increase in the up-regulation of Suf system genes was observed (Table 5.9). This was due to the activation of bacterial defence system after the completion of one replication cycle by 30 min. time point, which in turn activated Suf system genes to maintain the bacterial homeostasis.

In order to maintain homeostasis through Suf system, L-Ag NPs exposure also induced the expression of cysteine biosynthesis genes. Cysteine is the most frequently present amino acid in the functional site of proteins and is prone to oxidation due to the presence of ROS, which is basically required for the assembly of Iron-Sulfer cluster complex (Poole, 2015). Cysteine biosynthesis genes are related to various processes involved in the functioning of *E. coli* viz. ABC family sulphate/thiosulphate transporter and other complementary processes essential for the reduction & assimilation of sulphate for the biosynthesis of cysteine (van der Ploeg et al., 1996 and 2001). Biosynthesis of cysteine in *E. coli* is achieved by three different precursor materials viz. sulfate, taurine and alkenosulfonates, which synthesize sulphite with the help of *cys*, *tauABCD* and *ssuABC* gene clusters, respectively (van der Ploeg et al., 2001). Sulphite is further converted to sulphide and finally to cysteine, which leads to synthesize Iron-sulfer cluster complex. Differential analysis of these gene cluster showed that most of the cysteine is synthesized by utilizing sulfate as a starting material whereas, taurine is utilized second after sulfate but alkenosulfonates was not utilized in case of L-Ag NPs treated *E. coli* K12. Differential expression analysis showed that 5 min. post L-Ag NPs exposure resulted in the maximum up-regulation of *cys* and *tauABCD* gene clusters. At 30 min. time point, a decrease was observed in the up-regulation of *cys* gene cluster, whereas, non-significant expression was observed for *tauABCD* gene cluster (Table 5.10). This decrease in the expression of these genes at 30 min. time point can be correlated with the activation of bacterial defence system. Similarly, McQuillan et al. (2014) also studied the differential analysis of cysteine biosynthesis genes after exposure to silver species for 10 min. and reported up-regulation of *cys* gene cluster.

Table 5.10: Differential expression profile of genes related to cysteine biosynthesis mechanism under the stress of L-Ag NPs.

Gene ID	Gene name	Log_2 fold change		Protein annotation
		5 min.	30 min.	
b2422	*cysA*	6.91253	1.646965	Sulfate/thiosulfate ABC transporter ATP binding subunit
b1275	*cysB*	2.050239	NSE	DNA-binding transcriptional dual regulator CysB
b2750	*cysC*	6.713937	1.240752	Adenylyl-sulfate kinase
b2752	*cysD*	7.706878	1.99553	Sulfate adenylyltransferase subunit 2

b3368	*cysG*	NSE	0.242896	Siroheme synthase
b2762	*cysH*	6.435186	1.271674	Phosphoadenosine phosphosulfate reductase
b2763	*cysI*	6.498862	1.348711	Sulfite reductase, hemoprotein subunit
b2764	*cysJ*	5.757814	0.940998	Sulfite reductase, flavoprotein subunit
b2414	*cysK*	3.660875	1.362608	O-acetylserine sulfhydrylase A
b2421	*cysM*	3.278069	-0.70145	Cysteine synthase B
b2751	*cysN*	6.462976	1.478365	Sulfate adenylyltransferase subunit 1
b2425	*cysP*	5.811883	1.188524	Thiosulfate/sulfate ABC transporter periplasmic binding protein CysP
b2424	*cysU*	6.213985	1.180588	Sulfate/thiosulfate ABC transporter inner membrane subunit CysU
b2423	*cysW*	6.713576	1.641552	Sulfate/thiosulfate ABC transporter inner membrane subunit CysW
b2413	*cysZ*	NSE	1.025844	Sulfate:H(+) symporter
b0365	*tauA*	2.157449	NSE	Taurine ABC transporter periplasmic binding protein
b0366	*tauB*	2.087739	NSE	Taurine ABC transporter ATP binding subunit
b0367	*tauC*	1.069549	NSE	Taurine ABC transporter membrane subunit
b0368	*tauD*	1.228615	NSE	Taurine dioxygenase

Under the oxidative stress conditions, bacteria also activate its efflux pump machinery to pump out the surplus intracellular silver ions (Gurbanov et al., 2018). As discussed in Chapter 4, bacteria activate two copper efflux machineries viz. cusCFBA and cue system, in response to exposure to silver. These machineries have been reported to show homology with the silver resistance system (*silCFBA*) of plasmid pMG101 (Gupta et al., 2001). Functioning of these regulons have been discussed in Chapter 4 (Fig. 4.15 A and 4.16 A). Differential gene expression analysis of these regulons showed that most of the genes have got maximum up-regulation at 5 min. post L-Ag NPs exposure. At 30 min. time point a decrease was observed in their up-regulation (Table 5.11). Decrease in the expression of these genes at 30 min. time point may be due to the removal of most of silver ions from bacterial cells by this time point. The *cusC* gene, a part of *cusCFBA* operon was found to be highest up-regulated gene among all the differentially expressed genes at 5 min. and 30 min., which suggests that activation of Cu^{+} efflux machineries play a pivotal role under the stress of L-Ag NPs. This kind of increase

in the gene expression of efflux pumps genes was also reported by the McQuillan et al. (2014), where differential gene expression of *E. coli* was studied by the microarray analysis.

Table 5.11: Differential expression profile of genes related to efflux pump regulation mechanism under the stress of L-Ag NPs.

Gene ID	Gene name	Log_2 fold change		Protein annotation
		5 min.	30 min.	
b0572	*cusC*	9.424468	8.689086	Copper/silver export system outer membrane channel
b0573	*cusF*	7.931478	6.66849	Copper/silver export system periplasmic binding protein
b0574	*cusB*	7.625627	6.349522	Copper/silver export system membrane fusion protein
b0575	*cusA*	5.528525	4.522279	Copper/silver export system RND permease
b0571	*cusR*	2.403519	1.21931	DNA-binding transcriptional activator CusR
b0570	*cusS*	1.98474	1.090907	Sensory histidine kinase CusS
b0484	*copA*	8.239259	7.30597	Cu^+ exporting P-type ATPase
b0123	*cueO*	6.752764	5.101303	Cuprous oxidase/multicopper oxidase with role in copper homeostasis
b0487	*cueR*	0.399519	0.524391	DNA-binding transcriptional dual regulator CueR

We were thereafter interested to understand whether silver causes the metabolic inactivation of bacteria or not? To understand this, we performed the differential gene expression analysis of the toxin-antitoxin (TA) system. It is a set of two or more closely linked genes, which encode a toxin and its corresponding antitoxin protein. This system in basically involved in the stabilization of genome, stress tolerance, phage protection etc. (Rowe-Magnus et al., 2003; Fineran et al., 2009; Diago-Navarro et al., 2010). In *E. coli*, eight TA systems are well characterized till date viz. MazF–MazE, RelE–RelB, ChpBK–ChpBI, YafQ–DinJ, YoeB–YefM, HipA–HipB, YafO–YafN and MqsR– MqsA (Yamaguchi and Inouye, 2011). Among all these, mazEF system is the most studied system (Amitai et al., 2004). Detailed explanation about the functioning of mazEF system has been discussed in Chapter 4 (Figure 4.17 A). Differential gene expression analysis of all the above mentioned TA systems showed either statistically non-significant or neutral gene expression under the exposure of L-Ag NPs at both

5 and 30 min. time points which suggests the metabolically active cell under the treatment of MIC_{75} of L-Ag NPs (data not shown).

Figure 5.4 represents the heat map of comparative differential expression of genes of all the tested pathways under the exposure of L-Ag NPs for 5 and 30 min. time points.

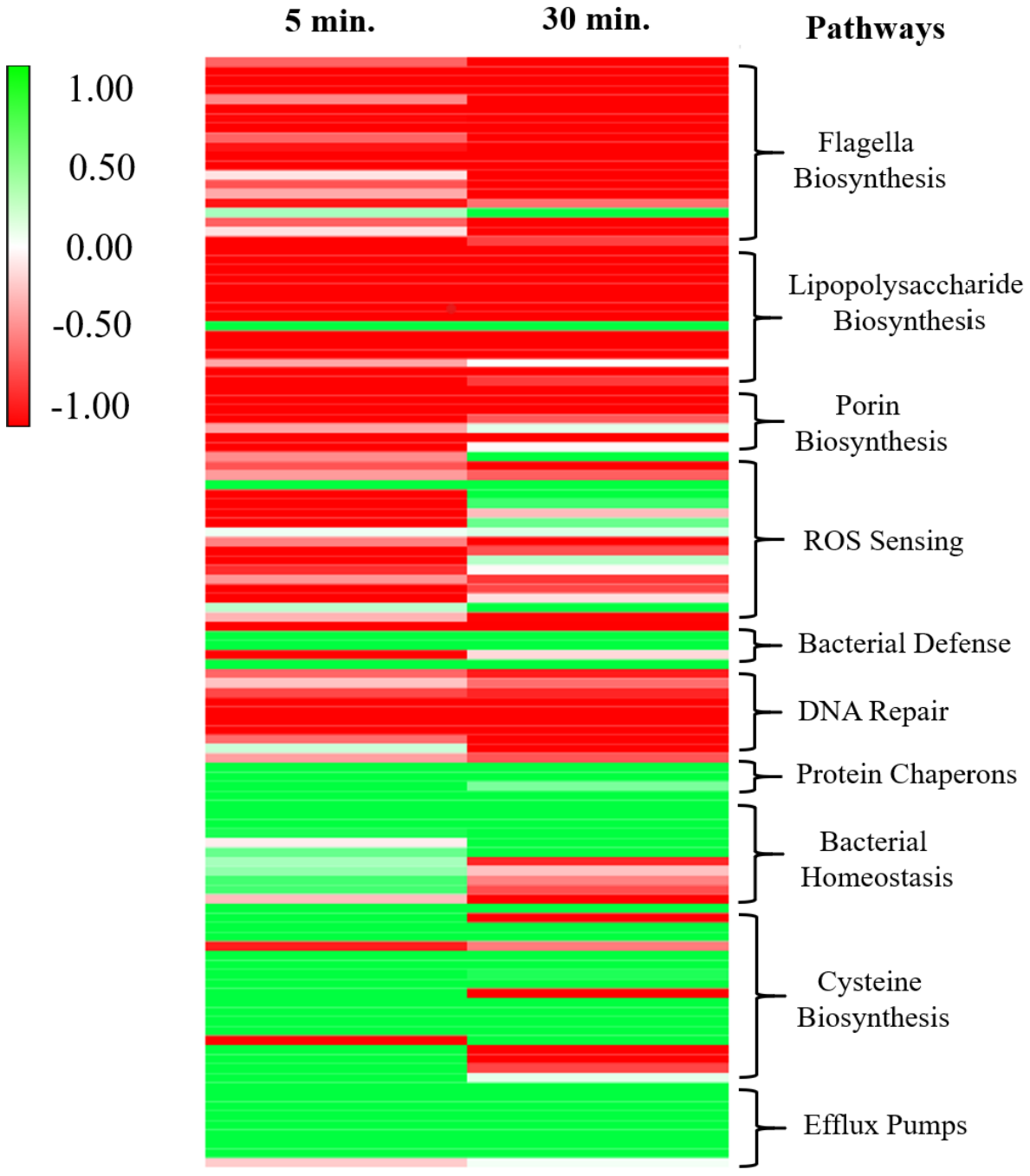

Figure 5.4: Heat map showing expression changes of key genes related to major pathways. The sequence of genes is similar as given in respective table numbers (5.2 to 5.11) (Green and red colour denote the up-regulated and down-regulated genes, respectively).

Gene Ontology (GO) classification analysis of differentially expressed gene was performed to find out the functional categorization of gene products according to their biological processes, cellular components, and molecular functions. GO enrichment pathway and GO biological process (GOBP) terms describe the biological role of genes and their respective molecular functions. The GO classification is a collective effect to deliver information on gene product descriptions from various databases (van Aerle et al., 2013; Sun et al., 2017). GO enrichment pathway analysis was performed separately for the 5 and 30 min. time points post treatment. It showed the up-regulation of 17 and 14 biological processes at 5 min. and 30 min. post L-Ag NPs exposure, respectively (Figure 5.5). Likewise, down-regulation of 10 and 14 biological processes were observed for the 5 and 30 min. time points, respectively (Figure 5.6). The data for cellular component and molecular functions are not shown.

In case of GOBP term analysis, in total 25 and 117 terms were found to be up-regulated at 5 and 30 min. post L-Ag NPs exposure, respectively (Figure 5.7 A and B). Whereas, 25 and 33 terms were found to be down-regulated at 5 and 30 min. post L-Ag NPs exposure, respectively (Figure 5.8 A and B).

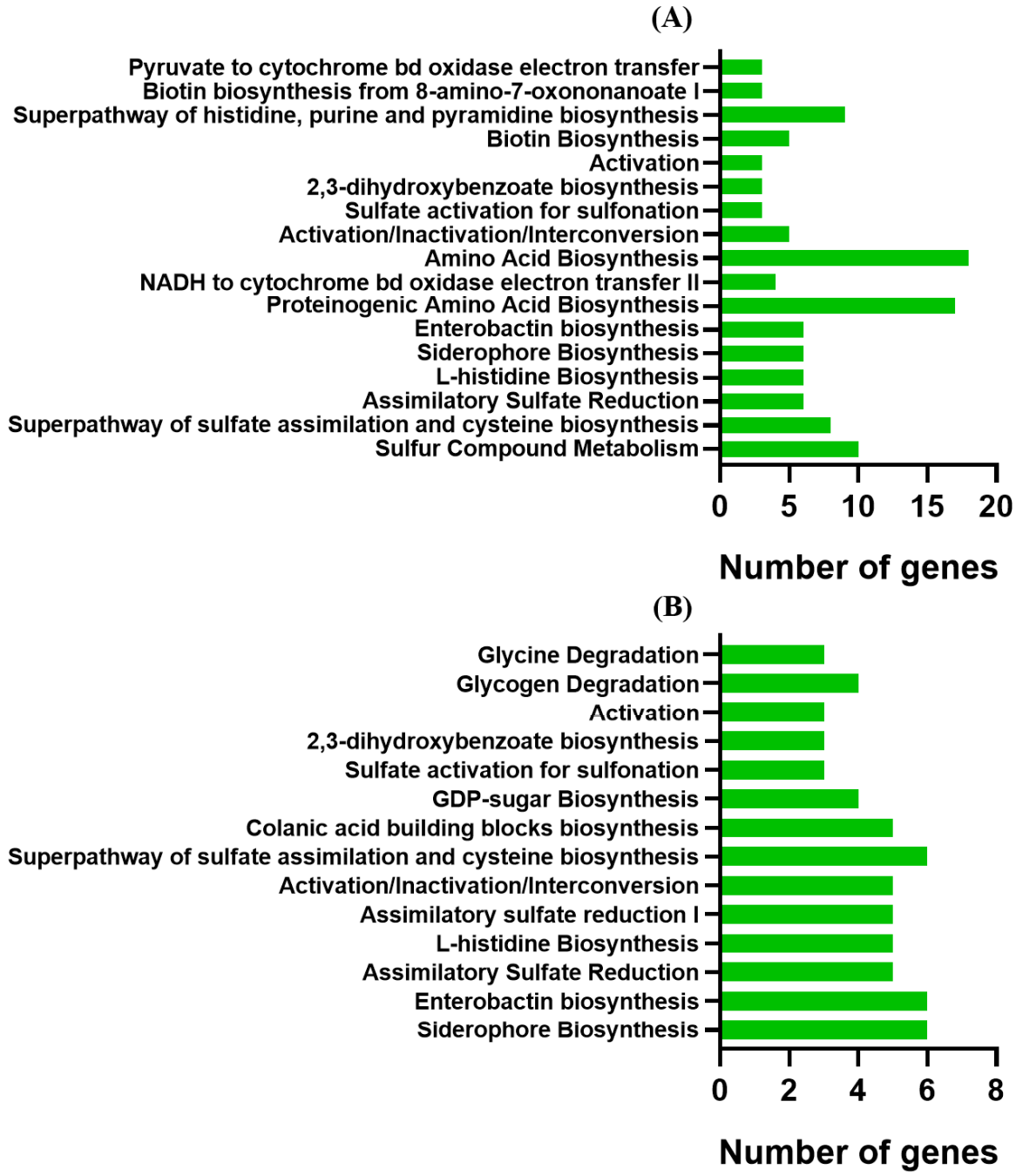

Figure 5.5: GO enrichment analysis showing the up-regulated biological processes at (A) 5 min. and (B) 30 min.

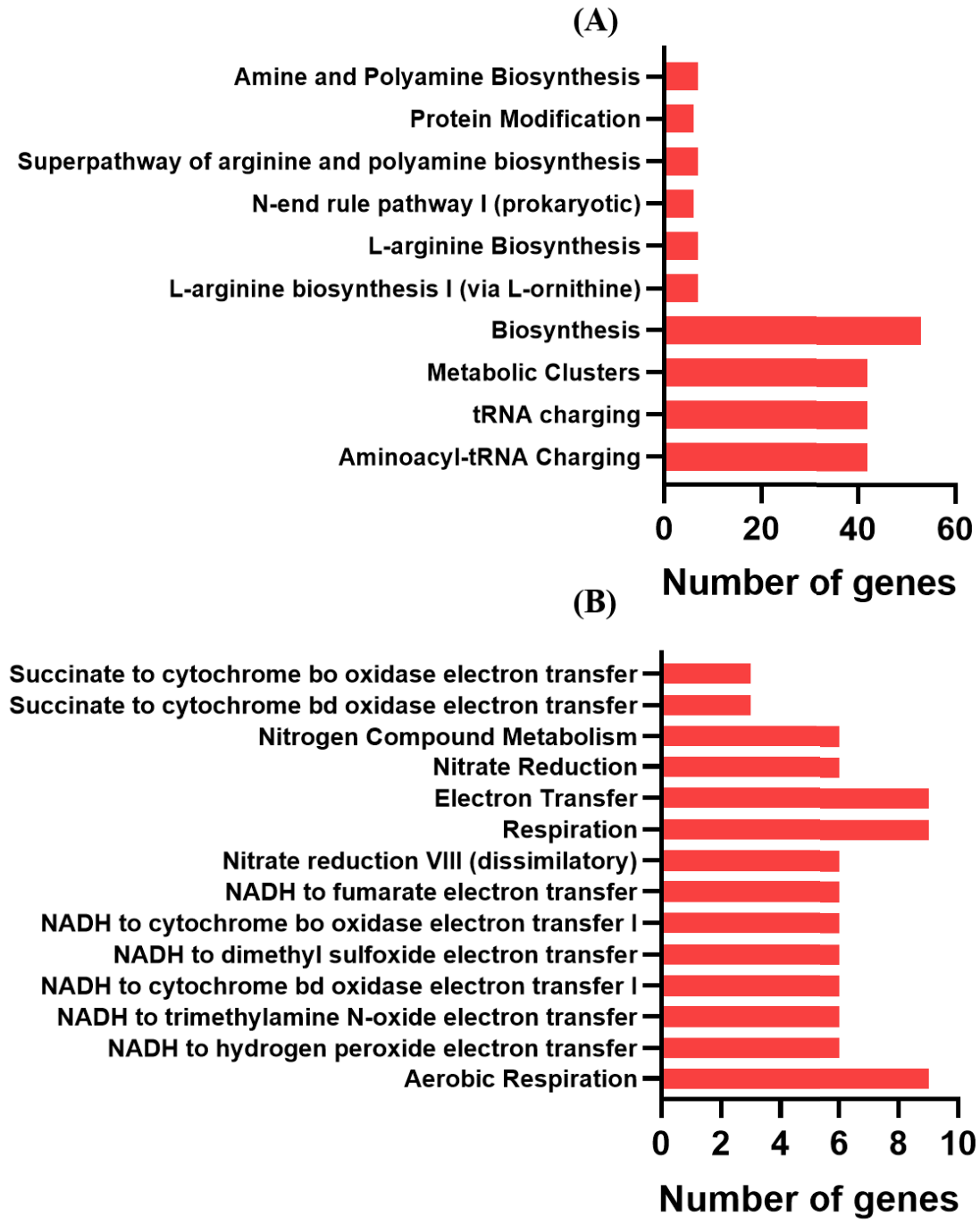

Figure 5.6: GO enrichment analysis showing the down-regulated biological processes at (A) 5 min. and (B) 30 min.

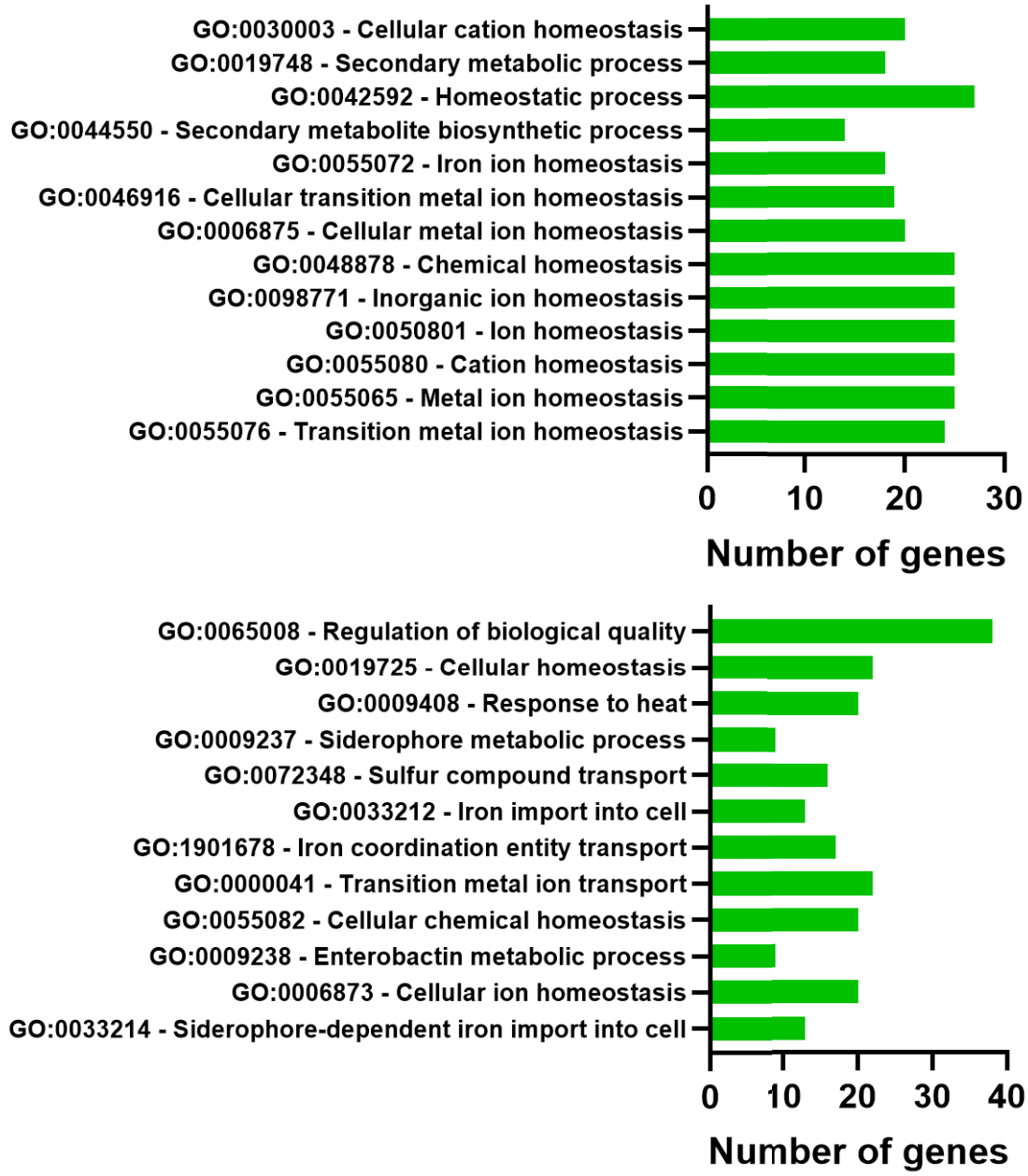

Figure 5.7 A: GOBP term analysis showing the up-regulated biological processes at 5 min.

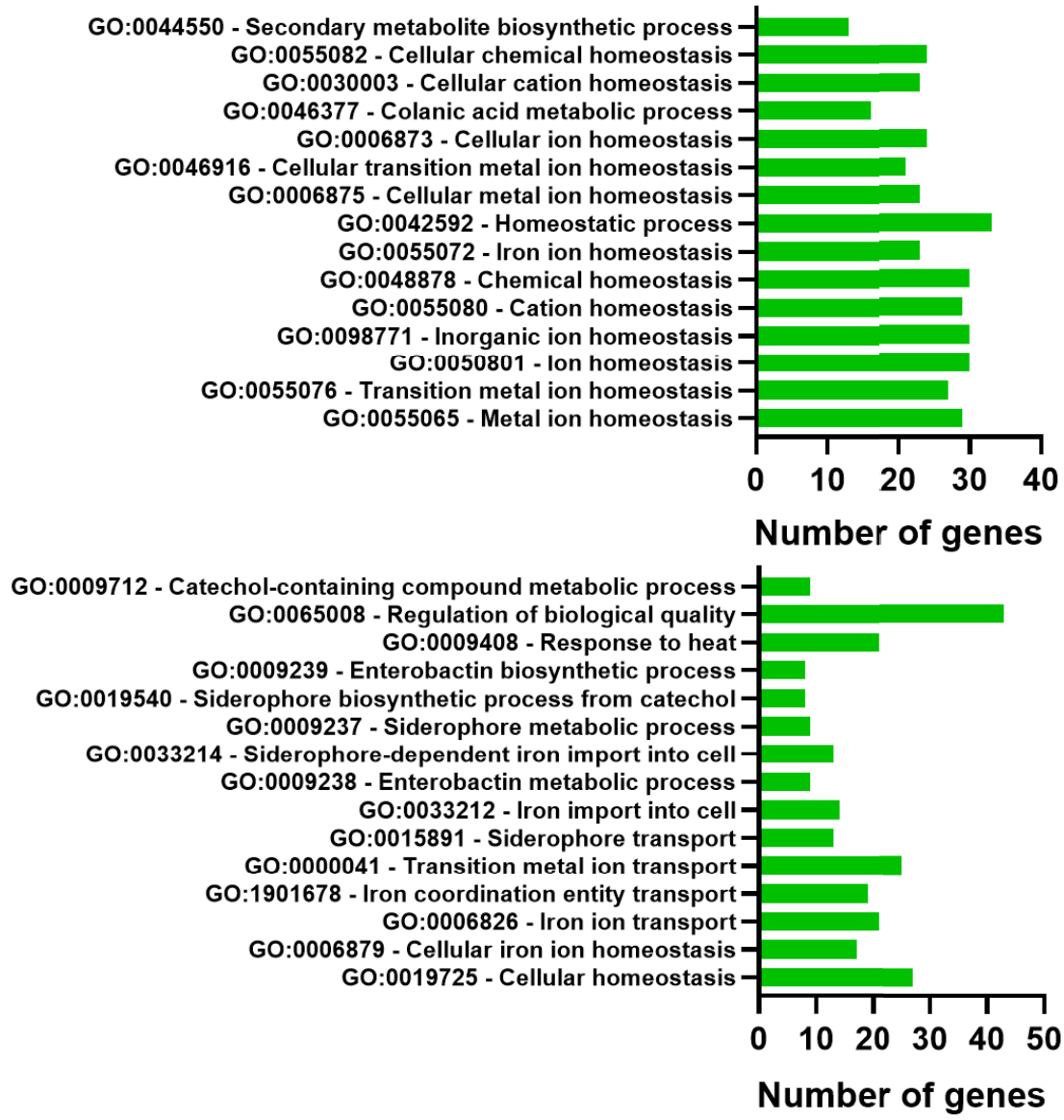

Figure 5.7 B: GOBP term analysis showing the up-regulated biological processes at 30 min.

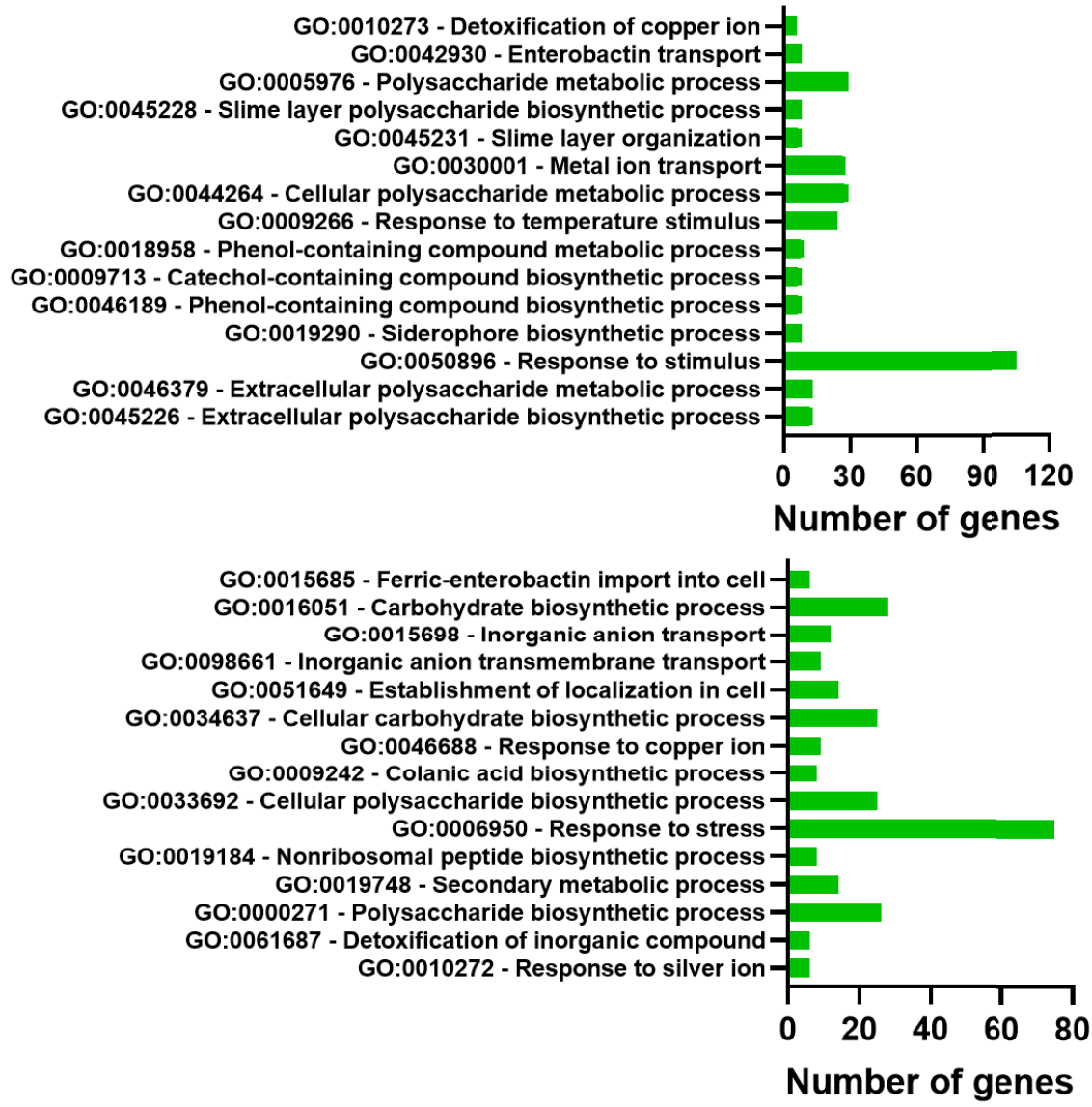

Figure 5.7 B: GOBP term analysis showing the up-regulated biological processes at 30 min. (Continued).

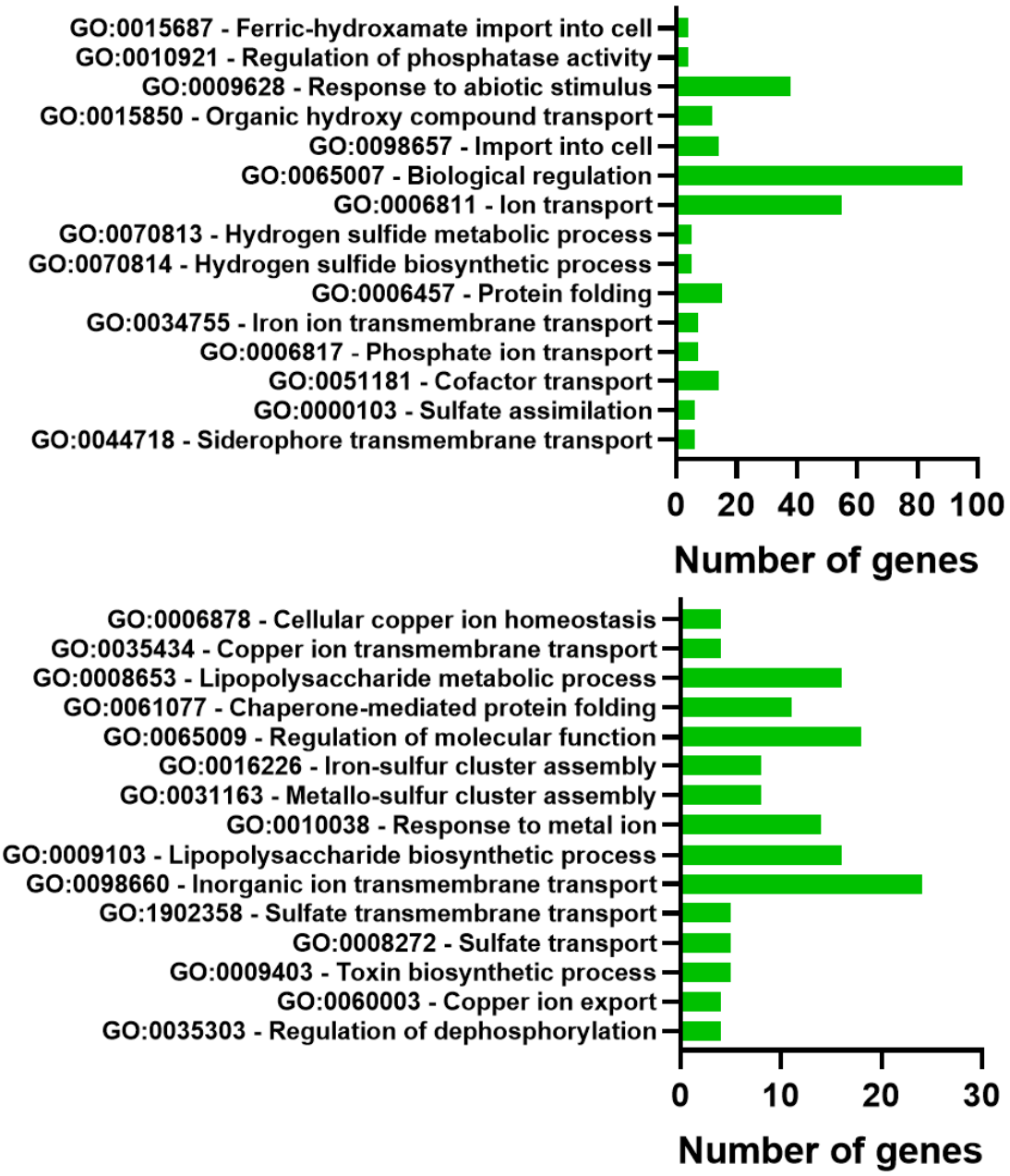

Figure 5.7 B: GOBP term analysis showing the up-regulated biological processes at 30 min. (Continued).

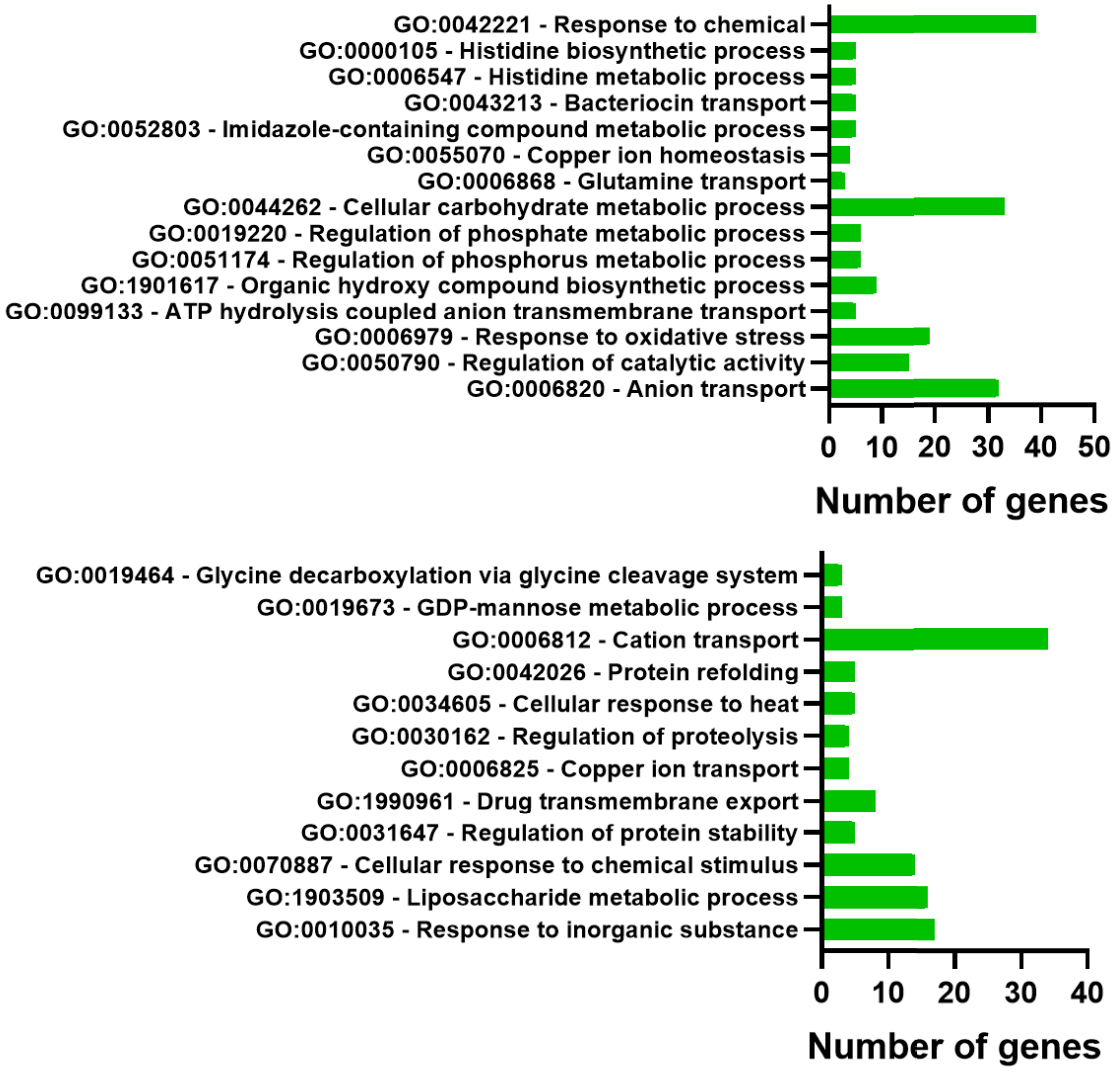

Figure 5.7 B: GOBP term analysis showing the up-regulated biological processes at 30 min. (Continued).

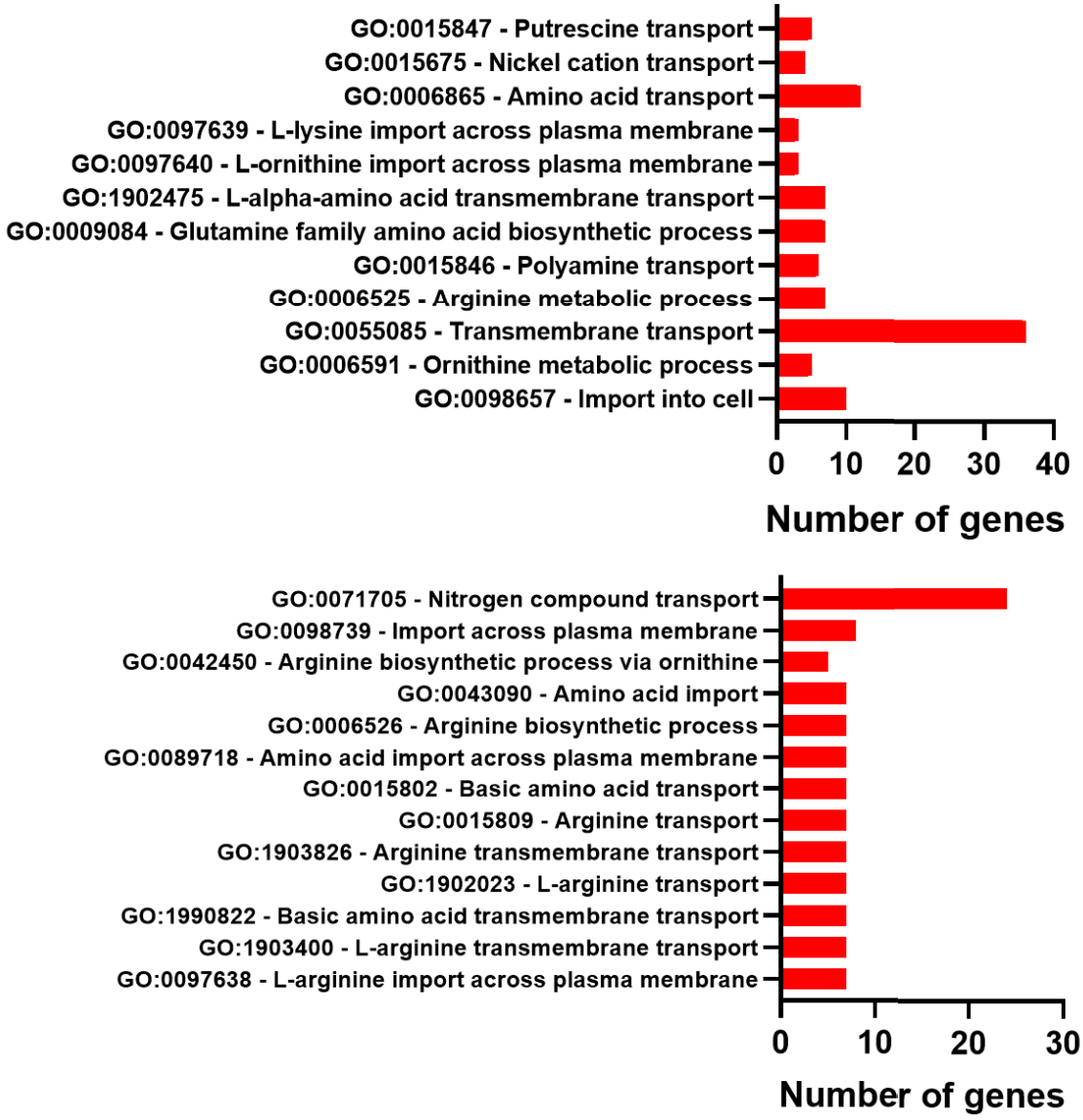

Figure 5.8 A: GOBP term analysis showing the down-regulated biological processes at 5 min.

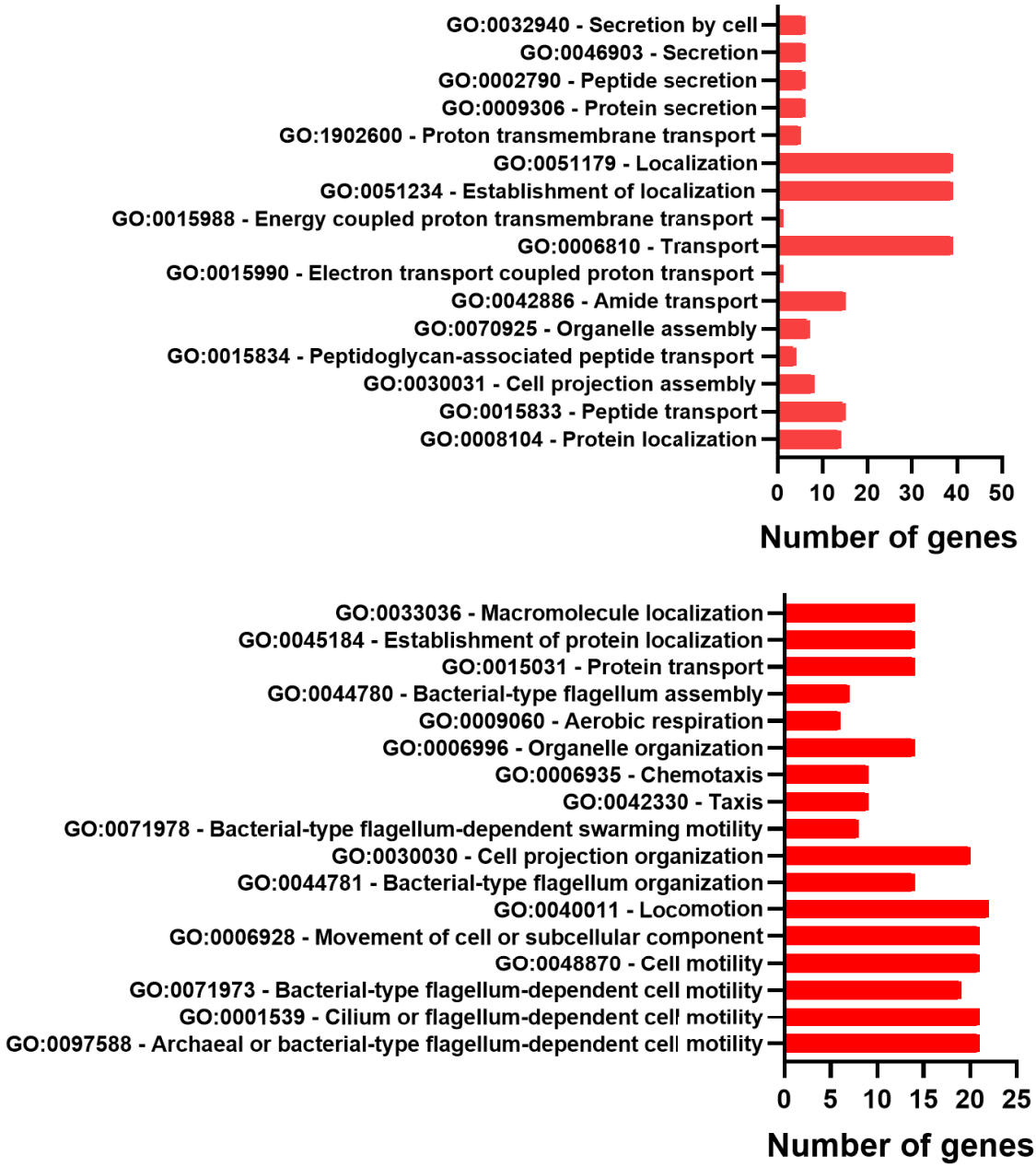

Figure 5.8 B: GOBP term analysis showing the down-regulated biological processes at 30 min.

The GO classification results were found to be in alignment with the transcriptomic results obtained by $\log_2$ fold change analysis. It was observed that the bacterial homeostatic pathways like cellular cation homeostasis, iron ion homeostasis, cellular transition metal ion homeostasis, inorganic ion homeostasis, which helps in the maintenance of bacterial homeostasis under the redox stress conditions get up-regulated at 5 min. time point. In addition, pathways related to siderophore metabolic process, enterobactin metabolic process also found to be up-regulated, which in turn help in upkeeping the bacterial homeostasis. At 30 min. post L-Ag NPs exposure, 117 different biological processes were found to be up-regulated which

also include the up-regulated biological processes at 5 min. time point. These include processes like response to silver ions and redox stress, carbohydrate and polysaccharide biosynthesis, copper ions homeostasis, Iron-sulfur cluster assembly, etc. Down-regulation of processes related to the transport of amino acid, nitrogen compound, polyamines, etc. was observed at 5 min. post L-Ag NPs exposure whereas processes related to chemotaxis, protein localization and transport, cell projection organization, electron transport chain, etc. were found to be down-regulated at 30 min. These results are in alignment with the outcomes of log_2 fold change in the bacterial transcriptome.

5.3.2 Validation of RNAseq data by qRT-PCR

For the validation of transcriptomic results, qRT-PCR data of some of the important genes related to bacterial defence system (*soxS*), efflux pump (*cusC and copA*), homeostasis (*sufB*), DNA repair mechanism (*recA*), and protein repair mechanism (*dnaK*) were used to validate the results obtained by RNAseq (Figure 5.9) Gene expression analysis by qRT-PCR reflected similarity to the RNAseq based transcriptomic data, which further support the strength of RNAseq based whole transcriptomic analysis.

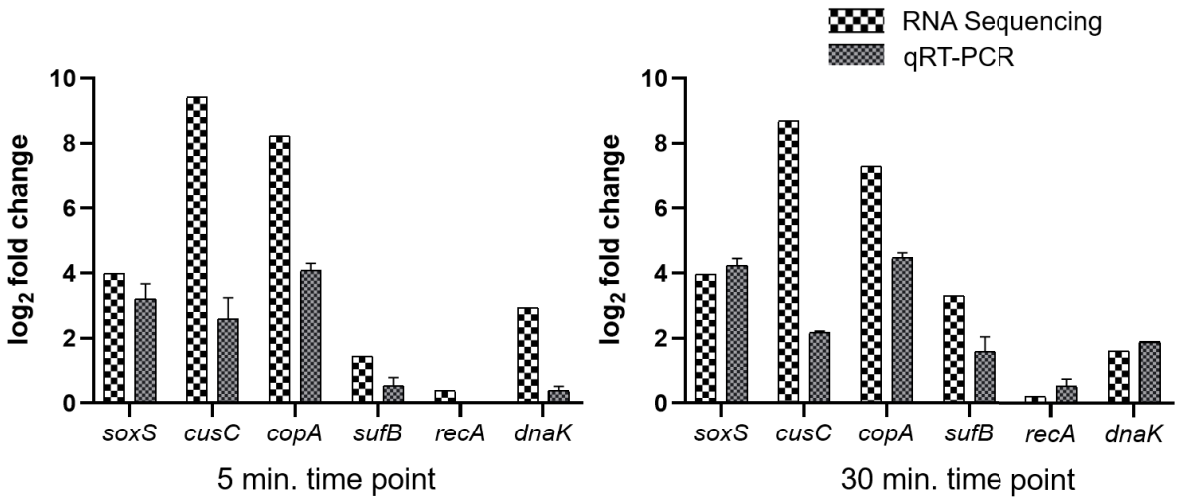

Figure 5.9: Validation measurements comparing the RNAseq and qRT-PCR data at 5 and 30 min, post L-Ag NPs exposure. Vertical bar represents SD.

5.3.3 Transmission electron microscopy (TEM) of bacterial cell

Damage to the cell integrity and structure of bacterial cells was visualized by TEM imaging. The untreated cells (control) revealed typical rod-shaped structure of *E. coli* K12 with smooth cell periphery having intact cell wall with no signs of aberration (Figure 5.10 A). No visible changes were observed in the morphology and structure of bacterial cells exposed to L-Ag NPs (Figure 5.10 B and C). This is in corroboration with the results obtained during the biochemical assays of membrane damage analysis, as discussed in Chapter 4. Multiple spot EDS analysis of bacterial surface showed absence of silver as no characteristic optical absorption band at 3.0 was observed. However, peaks for carbon and copper were clearly observed at 1.76, 0.24 and 0.92 keV, respectively, which was due to the use of carbon-coated copper grid for the sample preparation (Figure 5.10 D). The obtained results are in close agreement with the results of biochemical assay, qRT-PCR, and RNAseq analysis.

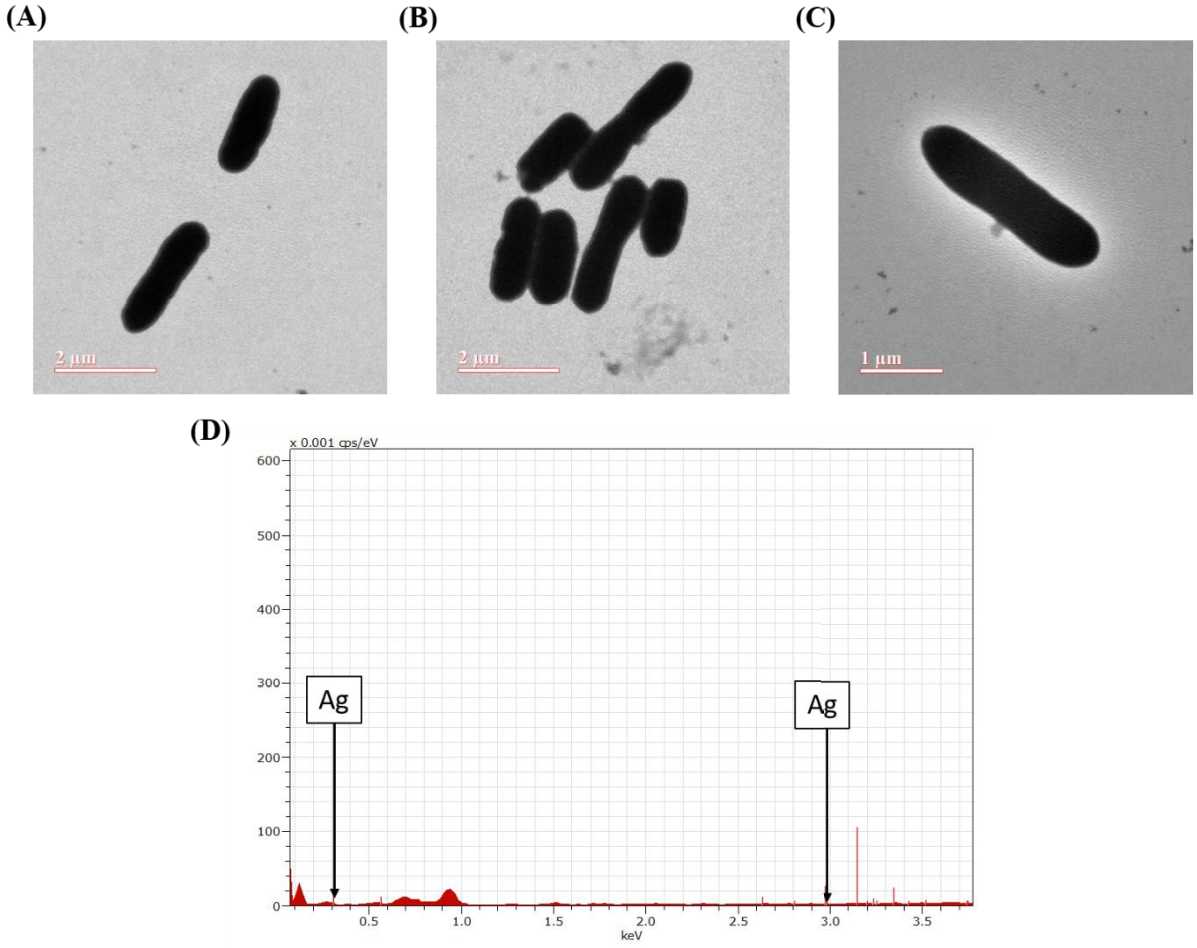

Figure 5.10: TEM micrograph of *E. coli* K12 exposed to L-Ag NPs (A) control (without exposure), (B and C) MIC_{75} of L-Ag NPs [6.75 µg (Ag) mL^{-1}], and (D) Spot EDS analysis of bacterial cell surface.

5.4 Conclusion

This chapter deals with the transcriptomic profiling of *E. coli* K12 exposed to MIC_{75} of L-Ag NPs for 5 and 30 min., by high throughput RNA sequencing technique. RNAseq of *E. coli* K12 showed a high number of total reads along with significant ratio of high-quality reads, which confirmed the excellent quality and quantity of the obtained RNAseq data. Total 4344 genes were found to be differentially regulated, out of which 2164 and 2285 genes were found to be statistically significant at 5 min. and 30 min. time points, respectively. To elucidate the complete antibacterial action of L-Ag NPs, various biological pathways were analysed based on their probable role under the stress of silver species. The obtained RNAseq data were found to be consistent with that of qRT-PCR analysis discussed in Chapter 4.

The down regulation of genes related to porin proteins and neutral behavior of LPS biosynthesis genes, showed the entry of silver ions released from L-Ag NPs through porin proteins. RNAseq. data confirmed the generation of ROS in the form of hydrogen peroxide radicals and showed active involvement of *soxRS* to sense the oxidative stress and in turn activate the defense mechanism. In response to oxidative stress, *E. coli* K12 cells activated the alternate mechanism (Suf system) to maintain the cellular homeostasis along with cysteine biosynthesis machinery. To remove the surplus silver ions from the bacterial cytoplasm, Cu^{+}/Ag^{+} specific efflux machineries like CusCFBA and Cue systems got activated. The expression of *cusC* gene was found to be maximum among all the differentially expressed genes, which suggest that overuse of Ag NPs can lead to the development of silver resistance in bacterial cells. We further explored the gene pathways and biological processes of *E. coli* K12 upon exposure to L-Ag NPs. The obtained results suggested the up-regulation of bacterial homeostatic pathways viz. cellular cation homeostasis, iron ion homeostasis, cellular transition metal ion homeostasis, inorganic ion homeostasis, which helps in maintenance of bacterial homeostasis under the redox stress conditions. In addition, pathways related to siderophore metabolic process and enterobactin metabolic process also got upregulated, which in turn helps in upkeeping the bacterial homeostasis. Moreover, upregulation of biological processes like response to silver ions and redox stress, carbohydrate and polysaccharide biosynthesis process, copper ions homeostasis process, iron-sulfur cluster assembly and many more was observed. Overall, this study elucidates the complete antibacterial mechanism of L-Ag NPs against *E. coli* K12. Considering the use of silver and silver based products as antibacterial agents in the current era, further studies need to be done on the development of silver resistance in bacterial cells.